

Siderophores and the formation of cerium anomalies in anoxic environments

D. Kraemer, M. Bau

Supplementary Information

The Supplementary Information includes:

- Supplementary Methods and Samples
- Tables S-1 to S-4
- Figures S-1 to S-9

Supplementary Methods and Samples

Samples

A set of igneous rocks ranging in composition from mafic to felsic was chosen for investigating water-rock interaction (WRI) in presence of siderophores at various redox levels. In order to facilitate comparison, most of the incubation experiments were conducted on aliquots of rock powders also used in earlier experiments by Kraemer *et al.* (2015) for DFOB incubation experiments under atmospheric conditions. In addition, a Silurian island-arc basalt from the Dingle Peninsula, Ireland, and an intra-plate ocean-island basalt from Hawaii (BHVO-2, issued by the USGS as certified reference material) were used in the experiments. The igneous rocks were chosen to also represent different textures and plate-tectonic settings. The total set comprises two mid-ocean ridge basalts (MORB), four ocean island basalts (OIB), one island-arc basalt and one island-arc andesite, and an intraplate granite. The mineralogical composition of some of the rocks has been described by Kraemer *et al.* (2015) and is shown in Table S-1. The MORB sample was collected from an aphyritic sheet flow near the Turtle Pits hydrothermal field at the Mid-Atlantic Ridge (Haase *et al.*, 2007). The interior microcrystalline basalt (MORB-TP) and the exterior basaltic glass (MORB-TP glass) were sampled separately. OIB-Me is a primitive aphanitic alkali basalt from Mehetia Island (Society hotspot) and is discussed as sample Me90-05 by Binard *et al.* (1993). The second OIB sample, OIB-Haw, is a vesicular tholeiite from Kilauea, Hawaii, and is also discussed by Giese and Bau (1994). The aphanitic island-arc basalt BIRN3 originates from the Clogher Head Formation of the Silurian Dunquin Group on the Dingle Peninsula, Ireland. Samples of more evolved mafic and intermediate composition are basaltic andesite OL-20b and andesite A-Jp. The basaltic andesite was originally described by Schnurr (1995) as a basaltic andesite originating from the Paleoproterozoic Ongeluk Formation of the Transvaal

Supergroup, South Africa. The island-arc andesite A-Jp originates from a lava flow underlying the Nishiki-numa spring (Hokkaido, Japan) (Bau *et al.*, 1998). The granite GSAF3 is from the Lebowa Granite Suite, Bushveld Complex, South Africa.

Concentration data (Table S-3) for the majority of the bulk rock samples and used herein for normalisation were taken from literature (Kraemer *et al.*, 2015).

Experimental

The leaching experiments (Table S-2) were done in multiple, independent batches named alphabetically from A to I. Batches labelled A-E, G, H and I involve desferrioxamine B (DFOB) as model siderophore, whereas desferrichrome (DFC) was used in batch F. Batches A and B were conducted as time-series experiments under anoxic conditions for ocean-island basalt BHVO-2 and granite GSAF3 and as 24 hr experiments for all other samples. Time intervals in anoxic batches A and B partially overlap as a mean to assess reproducibility. Experiments C, G and H are anoxic and hypoxic batches conducted independently of A and B also to evaluate reproducibility. The batches D and I are time-series experiments similar to A, but were conducted under hypoxic and oxic conditions, whereas E is a 24 hr experiment conducted under oxic conditions. Note that some of these are repetitions of the oxic experiments presented in Kraemer *et al.* (2015) and published data are shown for sample OL20-B for the oxic experiments due to insufficient amounts of sample powder left in the course of the experiments. Batch F consists of experiments conducted under anoxic, hypoxic and oxic conditions on ocean-island basalt BHVO-2 with the model siderophore DFC.

The experimental setup was modified after Kraemer *et al.* (2015). Except for BHVO-2 which is a certified reference material and issued already as rock powder by the United States Geological Survey, the rock samples were crushed, rinsed with DI and after drying ground with a Fritsch Pulverisette 6 planetary ball mill with agate mortar. Bulk decomposition of the powdered rock samples (including BHVO-2) was carried out using a Picotrace DAS acid digestion system (Pico Trace, Germany) following a mixed acid (HF-HNO₃-HCl) digestion protocol (Dulski, 2001). For the leaching experiments, the sample powders were gravimetrically weighed into acid-cleaned 50 to 250ml LDPE bottles matching a solid content of 20g/L. The batch leaching experiments were conducted in a trace metal-clean environment with acid-cleaned labware as follows:

Experiments conducted under oxic conditions

For the oxic experiments, the solutions were prepared and the experiments conducted under ambient conditions. De-ionised (DI) water was filled into acid-cleaned LDPE bottles at an appropriate amount. The siderophore desferrioxamine B (DFOB) was obtained in its mesylate form as the drug Desferal (Novartis AG) which consists of pure desferrioxamine-B mesylate and which is commonly used to treat acute and chronic iron overload (Bernhardt, 2007; Nick *et al.*, 2003). The purity of Desferal was checked by reagent blank measurements; trace-element concentrations in Desferal were found to be at least two orders of magnitude lower than the concentrations in our experiments. Desferrichrome was obtained as Fe-free powder ('Ferrichrome Iron-free from *Ustilago sphaerogena*'; CAS-No: 34787-28-5) from Sigma Aldrich. The DFOB or DFC powders were added to the DI water by gravimetrically weighing in appropriate amounts of the powders (matching a final molarity of 1 mmol/L DFOB/DFC), the bottle was closed and shaken to facilitate dissolution. The pH was measured separately in small plastic beakers to avoid potential contamination by the pH electrode.

Experiments conducted under hypoxic and anoxic conditions

The anoxic and hypoxic experiments were conducted completely inside an Anaerobic Chamber manufactured by Coy Laboratory Products (Grass Lake, Michigan, USA). For hypoxic conditions, an O₂ controller was used, which constantly measures the oxygen concentration in the chamber and either adds nitrogen gas or air to the chamber to reach the desired O₂ concentration. This operating mode can reach hypoxic levels down to 0.1 % O₂. For completely anoxic conditions, the chamber is first purged with N₂ until O₂ concentration approaches 0.1 %. Then the chamber is purged with a



hydrogen gas mix (5 % H₂, 95 % N₂; ‘forming gas’) until H₂ concentration in the chamber reaches at least 3 %. In presence of the palladium catalyst, the hydrogen reacts with the remaining oxygen inside the chamber and water molecules are formed. With this technique, anoxic conditions are achieved and can be kept constant by continuously adding forming gas at defined time intervals, so that the consumed H₂ is replenished, and anoxic conditions are maintained by ensuring that at least 3.5-4.5 % H₂ are in the atmosphere of the chamber. Note that the manufacturer of the chamber provides a working range of “0-5 ppmv O₂” to account for the accuracy of the oxygen probe and potential leakage. We emphasise that H₂ concentrations were kept high enough throughout the experiments so that any O₂ leakage into the chamber was minimised as good as possible and the O₂ probe actually showed readings of 0 ppmv throughout the whole experiments. Any O₂ leaking in would immediately be removed by reaction with H₂ to H₂O at the Pd catalyst. Leakage of ambient air into the chamber would also immediately be visible by sharply increasing humidity readings due to the H₂O formation in the chamber. However, these remained constant throughout the experiments.

Before the atmosphere was changed, all labware needed for the experiments was put inside the chamber to minimise contamination of the atmosphere with ambient air during the experiment, for example when the airlock is used. The chamber was sealed and purged with N₂ and forming gas to reach anoxic conditions of 0 ppmv as indicated by the oxygen probe inside the chamber. The bottle with DI water was opened and stirred with a magnetic stirrer for at least 12 hours at anoxic conditions in the anaerobic chamber to remove any dissolved oxygen from the solution. A multimeter with a free dissolved oxygen (FDO) probe was used to verify that the DI solution was free of dissolved oxygen (see Table S-2). For the anoxic experiments, the siderophore powder, which was weighed in into small plastic beakers under ambient conditions, was then added after equilibration with the solution and stirred for at least another hour. The FDO content was then verified again in separate aliquots. For the hypoxic experiments, the DI water was first stirred in a similar way under anoxic conditions until FDO reached 0.0 %. Then, some ambient air was added to the chamber to achieve and maintain an O₂ concentration of 0.1 % with the help of the O₂ controller. The DI solution was stirred for another 12 hours to equilibrate with the hypoxic atmosphere. Afterwards, the FDO was checked and DFOB or DFC were added to the solution. After stirring for at least another hour, FDO was verified again.

Apart from the procedures described above, all experiments followed the same protocol. The solutions containing exactly 1 mmol/L DFOB and 1 mmol/L DFC were added via graduated acid-cleaned plastic cylinders either inside (hypoxic, anoxic experiments) or outside (oxic experiments) of the chamber to the LDPE bottles containing the rock powders. The bottles were then closed and handshaken to facilitate suspension and put on an orbital shaker operated at 180 rpm. The bottles were covered with aluminium foil to minimise UV-induced decomposition of the organic ligands. After the designated time, the suspensions were filtered with acid-cleaned syringe filters with a membrane pore size of 0.2 µm into new acid-cleaned LDPE bottles. A ca. 1 ml aliquot was taken for the determination of pH before the remaining solution (ca. 24ml for the majority of the DFOB experiments, less for DFC experiments) was acidified with 1 ml HCl and 10 µl HF for stabilization. For the time-series experiments, 250 ml suspensions were used and 10 ml aliquots of the well-shaken sample were taken and filtered with a filter syringe at the desired time interval and the added amounts of HCl and HF were adapted. We emphasise that for the anoxic and hypoxic experiments, all described steps were conducted inside the chamber and that the oxygen concentrations, which were constantly monitored, remained at 0 ppmv throughout the anoxic and at 0.1 % O₂ during the hypoxic experiments. The solutions were only removed from the atmosphere after filtration and acidification. Solution pH was measured inside the chamber under hypoxic and anoxic conditions, respectively. After using the airlock or entering the chamber with the gloves, extra care was taken that O₂ concentrations reached 0 ppmv again before the start of any activities inside the chamber.

Control experiments without siderophores

In a previous study (Kraemer *et al.*, 2015), we indicated that 24 hr control experiments under oxic conditions without DFOB (only DI) were below the detection limit of the ICP-MS and demonstrated with control experiments with HCl and acetic acid that Ce anomaly formation only occurred in presence of the siderophore DFOB. Here, we conducted



additional control experiments with DI and 0.01 mol/L HCl (pH 2) under strictly anoxic conditions as laid out in the previous paragraph. The resulting REY_{BN} patterns are presented in Figure S-6. In contrast to the siderophore experiments, REY in the DI experiments were mostly below the detection limit after 5 min of leaching and after 24 hours of leaching detectable only in some experiments (MORB-TP cryst, MORB-TP glass, A-Jp, GSAF3). Neither the DI nor the HCl experiments produced any Ce_{BN} anomalies in the leachates.

Analytical & Reporting

All solutions were measured for their REY compositions with a Perkin Elmer NexION 350x ICP-MS coupled to an Apex 2 desolvating nebulizer by Elemental Scientific. Interference correction for the rare earth elements as employed in this study was modified after Dulski (1994).

REY patterns in the bulk rocks are shown as chondrite-normalised REY patterns (REY_{CN}). C1 chondrite data used for normalisation was obtained from Anders and Grevesse (1989). The REY concentrations in the leachates are normalised to the respective bulk rock REY concentrations (REY_{BN}) in order to illustrate the fractionation induced by siderophore leaching from the rock material.

Ce anomalies are reported as Ce_N/Ce_N^{*} (Eq. S-1, (Bau *et al.*, 1996)) and are calculated with C1-chondrite normalised values. As the bulk-rock REY patterns do not show any anomalous behaviour of Ce, the anomalies were calculated with chondrite-normalised values. The Ce_N/Ce_N^{*} ratio is a measure of the anomalous behaviour of Ce, with values below unity indicating negative, values above unity indicating positive anomalies against the normalisation standard (here: chondrite).

Equation S-1:

$$\frac{Ce_N}{Ce_N^*} = \frac{Ce_N}{(0.5 * La_N + 0.5 * Pr_N)}$$



Supplementary Tables

Table S-1 Mineralogical composition of some of the rock samples (taken from Kraemer *et al.*, 2015). The samples BHVO-2 and BIRN-3 (not listed) are typical microcrystalline basalts with no visible secondary alteration. Abbreviations: Ol = olivine, Px = Pyroxene, Cpx = clinopyroxene, Mt = titanomagnetite, Plg = plagioclase.

Sample	Mineralogy	Reference
OIB-Me	Ol and Cpx phenocrysts in a glassy matrix of Plg and Mt, no visible secondary minerals	Giese and Bau (1994)
OIB-Haw	Phenocrysts of Ol in a matrix of Plg, Cpx and glass, no visible secondary minerals	Giese and Bau (1994)
MORB-EPR	Ol, Plg and Px microcrystallites in a partially devitrified glassy matrix, no visible secondary minerals	Giese and Bau (1994)
MORB-TP	Microcrystalline Ol, Plg and Px, no visible secondary minerals	Kraemer <i>et al.</i> (2015)
A-Jp	Microcrystalline Plg, Cpx and minor Ol, no visible secondary minerals	Bau (1998)
OL20B	Phenocrysts of Plg and Cpx in a Px-dominated matrix, minor amounts of sericite, chlorite and clay minerals indicate small-scale rock alteration	Schnurr (1995)
GSAF3	Plg, Qtz, minor mica, no secondary minerals	Kraemer <i>et al.</i> (2015)



Table S-2 Overview of the different experimental setups / runs. Times marked with an asterisk indicate that these experiments were only done with BHVO-2 and GSAF3 (as longer time-series experiments). The desferrichrome experiments (batch F) were only conducted with BHVO-2. FDO was determined with a multimeter probe after solution equilibration inside the chamber as described in the methods part of this article.

Experiment	Reagent	Experiment time	Solid content	Oxygen concentration in anaerobic chamber	Free dissolved oxygen (FDO) saturation in DFOB solution
A	1 mmol/L DFOB	5 min*, 1 hr*, 4 hr*, 8 hr*, 24 hr	20 g/L	0 ppmv O ₂	0.0 %
B	1 mmol/L DFOB	5 min, 20 min*, 1 hr	20 g/L	0 ppmv O ₂	0.0 %
C	1 mmol/L DFOB	24 hr	20 g/L	0 ppmv O ₂	0.0 %
D	1 mmol/L DFOB	5 min*, 1 hr*, 4 hr*, 8 hr*, 24 hr	20 g/L	0.1 % O ₂	1.5 %
E	1 mmol/L DFOB	24 hr	20 g/L	21 % O ₂ (PAL)	100 %
F	1 mmol/L DFC	5 min, 24 hr	20 g/L	0 ppmv O ₂ 0.1 % O ₂ 21 % O ₂ (PAL)	0.0 % 1.4 % 100 %
G	1 mmol/L DFOB	5 min, 24 hr	20 g/L	0 ppmv O ₂	0.0 %
H	1 mmol/L DFOB	5 min, 24 hr	20 g/L	0.1 % O ₂	1.4 %
I	1 mmol/L DFOB	5 min*, 1 hr*, 4 hr*, 8 hr*, 24 hr*, 144 hr*	20 g/L	21 % O ₂ (PAL)	100 %



Table S-3 Bulk rock REY compositions of the igneous rocks used for leaching experiments, obtained from Kraemer *et al.*, 2015; except for BHVO-2 and BIRN3 (this study). All reported concentrations are in mg kg⁻¹.

Type	Mid-ocean ridge basalt	Mid-ocean ridge basalt	Ocean island tholeiitic basalt	Ocean island tholeiitic basalt	Ocean island alkali basalt	Ocean-island basalt	Basaltic andesite	Island-arc andesite	Granite
Locality	Atlantic Ridge Turtle Pit	Atlantic Ridge, Turtle Pit	Hawaii, Pacific Ocean	Hawaii, Pacific Ocean	Mehetia Island, Pacific Ocean	Dingle, Ireland	South Africa	Hokkaido, Japan	Bushveld, South Africa
Sample name	MORB-TP	MORB-TP glass	BHVO-2	OIB-Haw	OIB-Me	BIRN3	OL-20B	A-Jp	GSAF3
La	2.92	2.96	15.50	11.47	41.15	12.50	19.10	4.55	67.36
Ce	8.69	8.87	38.10	28.56	89.60	29.60	37.60	10.50	147.35
Pr	1.48	1.51	5.59	4.18	11.45	3.81	4.32	1.48	17.61
Nd	8.10	8.19	24.50	19.85	48.87	16.17	16.80	6.86	60.16
Sm	2.77	2.83	6.00	5.28	10.52	4.57	3.35	1.87	16.44
Eu	1.08	1.10	2.10	1.86	3.23	1.37	1.01	0.68	0.38
Gd	3.86	3.88	6.60	5.75	9.46	5.48	3.25	2.26	18.79
Tb	0.67	0.68	0.94	0.88	1.29	0.89	0.51	0.37	3.73
Dy	4.49	4.61	5.40	5.16	6.43	5.91	3.16	2.46	26.25
Y	25.80	26.10	25.30	24.26	27.00	33.60	18.00	13.94	160.70
Ho	0.96	0.98	0.98	0.97	1.06	1.16	0.67	0.54	5.41
Er	2.81	2.86	2.55	2.54	2.49	3.61	1.93	1.56	16.43
Tm	0.40	0.41	0.34	0.33	0.29	0.46	0.28	0.22	2.15
Yb	2.58	2.64	2.10	1.97	1.59	3.49	1.88	1.56	15.46
Lu	0.39	0.39	0.28	0.29	0.22	0.55	0.29	0.23	2.22
Ratios									
Y/Ho	26.79	26.63	25.82	25.01	25.47	28.97	26.91	25.81	29.70
Ce_{CN}/Ce_{CN}'	0.99	1.00	1.02	0.99	0.98	1.02	0.96	0.97	1.01

Table S-4 Data Table with leachate concentrations, calculated Ce anomalies, Y-Ho ratios and pH of the siderophore experiments.

Table S-4 is available for download as an Excel file in the online version of this article at <https://doi.org/10.7185/geochemlet.2227>.



Supplementary Figures

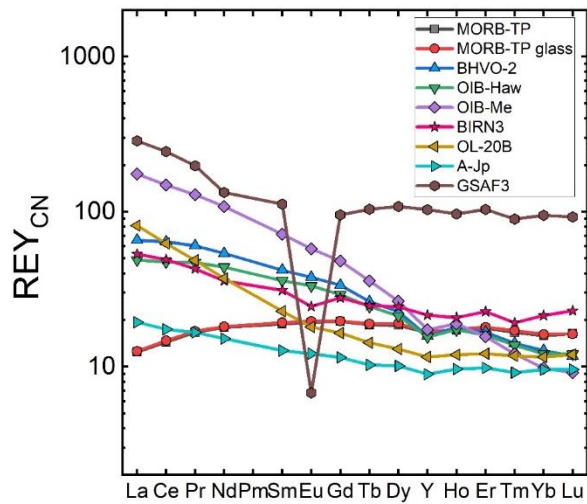


Figure S-1 Chondrite-normalised REY patterns of the bulk rock samples used for the leaching experiments. Note the absence of Ce_{CN} anomalies in all rock samples which could bias the bulk-rock normalised REY patterns of the leachates.

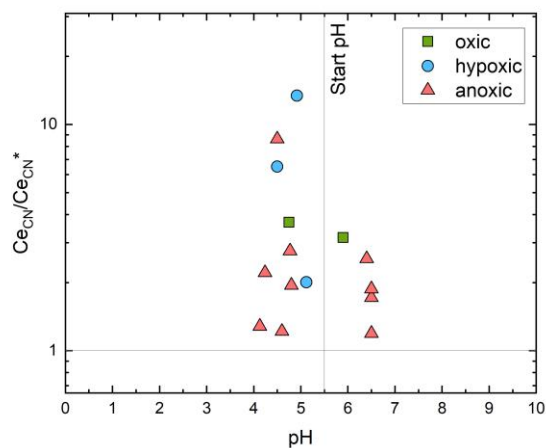


Figure S-2 Leachate pH versus Ce anomaly (expressed as Ce_{CN}/Ce_{CN}^*) of the leachates after 5 min of leaching in presence of siderophores.

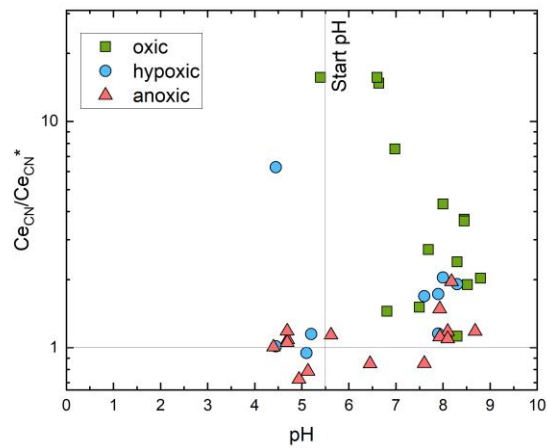


Figure S-3 Leachate pH versus Ce anomaly (expressed as Ce_{CN}/Ce_{CN}^*) of the leachates after 24 hours of leaching in presence of siderohores.

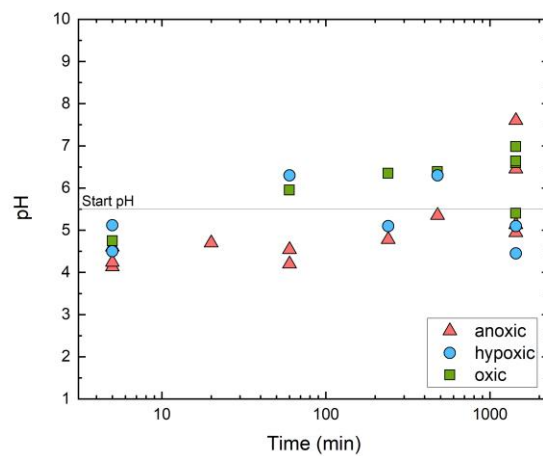


Figure S-4 pH versus time for the BHVO-2 siderophore experiments conducted under anoxic, hypoxic and oxic conditions.



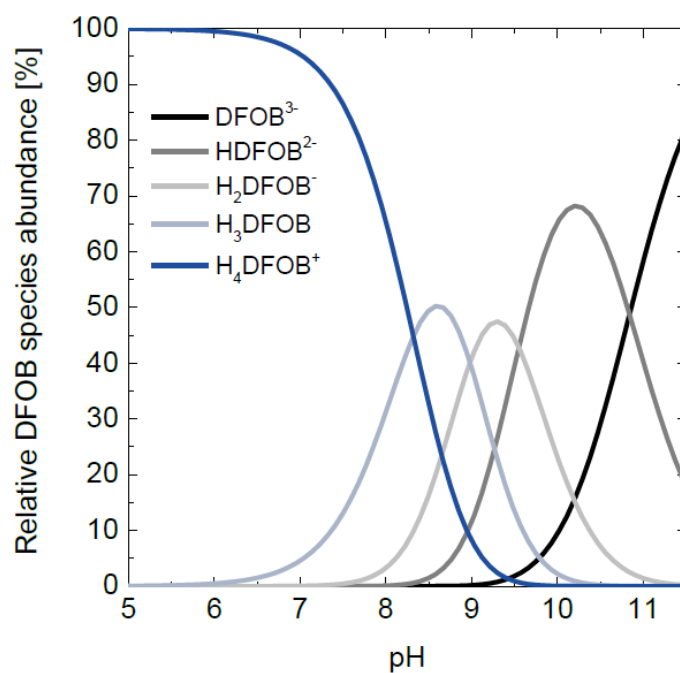


Figure S-5 Speciation curves for DFOB as calculated by HySS2009 modelling using constants of Martell and Smith (2001; $I = 0.1$, $T = 25$ °C).

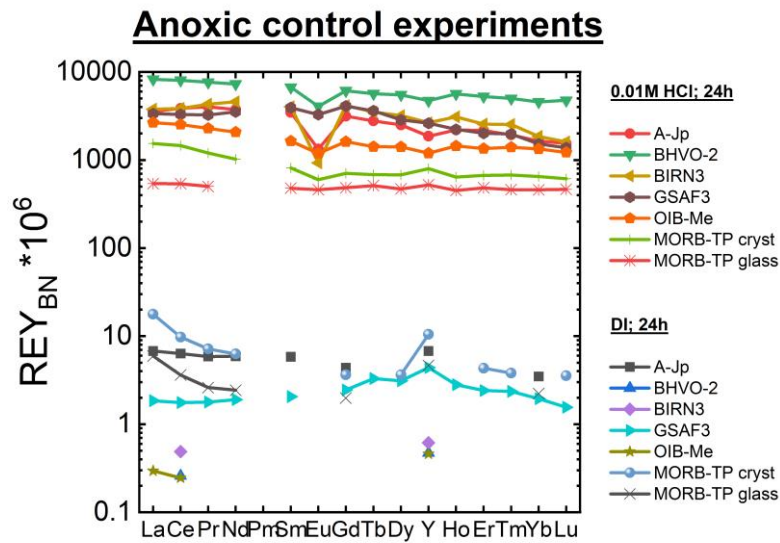


Figure S-6 Bulk rock-normalised REY patterns of control experiments (with DI and 0.01M HCl) conducted under anoxic conditions. Note the absence of Ce anomalies in all control experiments. Leachate REY concentrations for short-term DI leaching (<60 min) were below the detection limit and are not shown.

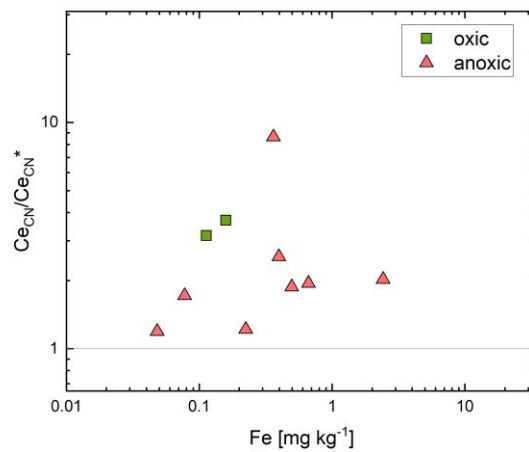


Figure S-7 Leachate Fe concentrations versus Ce anomaly (expressed as Ce_{CN}/Ce_{CN}^*) after 5 min of leaching with siderophores.

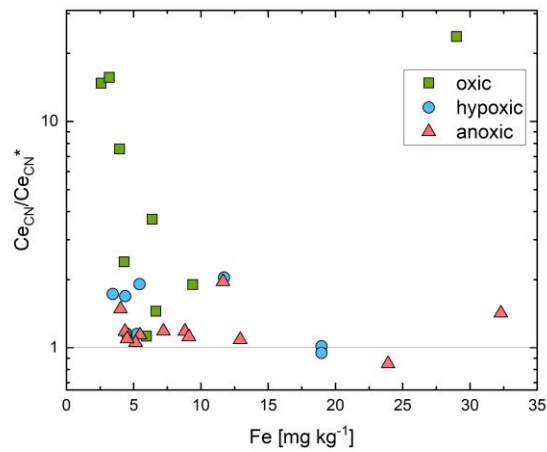


Figure S-8 Leachate Fe concentrations *versus* Ce anomaly (expressed as Ce_{CN}/Ce_{CN}^*) after 24 hours of leaching with siderophores.

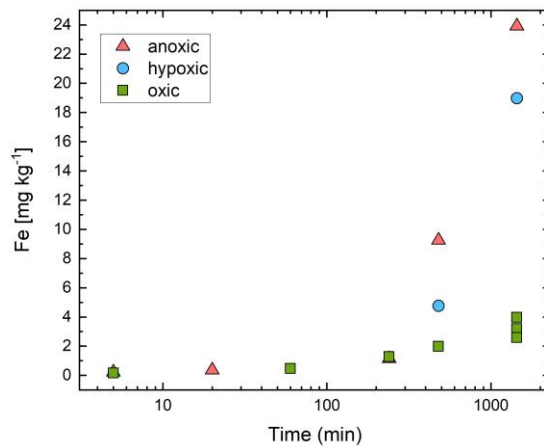


Figure S-9 Leachate Fe concentrations (in mg/kg) *versus* time for the BHVO-2 siderophore experiments conducted under anoxic, hypoxic and oxic conditions.



Supplementary Information References

- Anders, E., Grevesse, N. (1989) Abundances of the elements: Meteoritic and solar. *Geochimica et Cosmochimica Acta* 53, 197–214. [https://doi.org/10.1016/0016-7037\(89\)90286-X](https://doi.org/10.1016/0016-7037(89)90286-X)
- Bau, M., Koschinsky, A., Dulski, P., Hein, J.R. (1996) Comparison of the partitioning behaviours of yttrium, rare earth elements, and titanium between hydrogenetic marine ferromanganese crusts and seawater. *Geochimica et Cosmochimica Acta* 60, 1709–1725. [https://doi.org/10.1016/0016-7037\(96\)00063-4](https://doi.org/10.1016/0016-7037(96)00063-4)
- Bau, M., Usui, A., Pracejus, B., Mita, N., Kanai, Y., Irber, W., Dulski, P. (1998) Geochemistry of low-temperature water-rock interaction: Evidence from natural waters, andesite, and iron-oxyhydroxide precipitates at Nishikunuma iron-spring, Hokkaido, Japan. *Chemical Geology* 151, 293–307. [https://doi.org/10.1016/S0009-2541\(98\)00086-2](https://doi.org/10.1016/S0009-2541(98)00086-2)
- Bernhardt, P.V. (2007) Coordination chemistry and biology of chelators for the treatment of iron overload disorders. *Dalton Transactions* 30, 3214–3220. <https://doi.org/10.1039/b708133b>
- Binard, N., Maury, R.C., Guille, G., Talandier, J., Gillot, P.Y., Cotten, J. (1993) Mehetia Island, South Pacific: geology and petrology of the emerged part of the Society hot spot. *Journal of Volcanology and Geothermal Research* 55, 239–260. [https://doi.org/10.1016/0377-0273\(93\)90040-X](https://doi.org/10.1016/0377-0273(93)90040-X)
- Dulski, P. (1994) Interferences of oxide, hydroxide and chloride analyte species in the determination of rare earth elements in geological samples by inductively coupled plasma-mass spectrometry. *Fresenius' Journal of Analytical Chemistry* 350, 194–203. <https://doi.org/10.1007/BF00322470>
- Dulski, P. (2001) Reference Materials for Geochemical Studies: New Analytical Data by ICP-MS and Critical Discussion of Reference Values. *Geostandards Newsletter* 25, 87–125. <https://doi.org/10.1111/j.1751-908X.2001.tb00790.x>
- Giese, U., Bau, M. (1994) Trace element accessibility in mid-ocean ridge and ocean island basalt: an experimental approach. *Mineralogical Magazine* 58A, 329–330. <https://doi.org/10.1180/minmag.1994.58A.1.173>
- Haase, K.M., Petersen, S., Koschinsky, A., Seifert, R., Devey, C. W., Keir, R., Lackschewitz, K.S., Melchert, B., Perner, M., Schmale, O., Süling, J., Dubilier, N., Zielinski, F., Fretzdorff, S., Garbe-Schönberg, D., Westernströer, U., German, C.R., Shank, T.M., Yoerger, D., Giere, O., Kuever, J., Marbler, H., Mawick, J., Mertens, C., Stöber, U., Walter, M., Ostertag-Henning, C., Paulick, H., Peters, M., Strauss, H., Sander, S., Stecher, J., Warmuth, M., Weber, S. (2007) Young volcanism and related hydrothermal activity at 5°S on the slow-spreading southern Mid-Atlantic Ridge. *Geochemistry, Geophysics, Geosystems* 8. <https://doi.org/10.1029/2006GC001509>
- Kraemer, D., Kopf, S., Bau, M. (2015) Oxidative mobilization of cerium and uranium and enhanced release of “immobile” high field strength elements from igneous rocks in the presence of the biogenic siderophore desferrioxamine B. *Geochimica et Cosmochimica Acta* 165, 263–279. <https://doi.org/10.1016/j.gca.2015.05.046>
- Martell, A., Smith, R. (2001) *NIST Stability Constants of Metal Complexes Database 46, 6.0*. Gaithersburg, MD.
- Nick, H., Acklin, P., Lattmann, R., Buehlmayer, P., Hauffe, S., Schupp, J., Alberti, D. (2003) Development of Tridentate Iron Chelators: From Desferrithiocin to ICL670. *Current Medicinal Chemistry* 10, 1065–1076. <https://doi.org/10.2174/0929867033457610>
- Schnurr, W. (1995) Spurenelementgeochemie proterozoischer Cherts, Jasper and Jaspilite der Ongeluk Lava und der basalen Hotazel Formation, Kaapvaal Kraton, Südafrika. Diploma Thesis, RWTH Aachen.

